Food Structure 41 (2024) 100381

Contents lists available at ScienceDirect

Food Structure

journal homepage: www.elsevier.com/locate/foostr

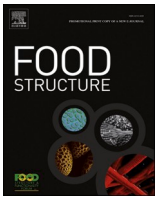

Cell wall permeability in relation to in vitro starch digestion of pea cotyledon cells

Abayomi Ajala [a,b], Lovedeep Kaur [a,b], Sung Je Lee [a], Patrick J.B. Edwards [a], Jaspreet Singh [a,b,*]

[a] School of Food Technology and Natural Sciences, Massey University, Private Bag 11 222, Palmerston North 4442, New Zealand
[b] Riddet Institute, Massey University, Private Bag 11 222, Palmerston North 4442, New Zealand

ARTICLE INFO

Keywords:
Cell wall
Cotyledon cells
Diffusion coefficient
PFG NMR
Pulses
Starch digestion
Water permeability

ABSTRACT

The role of cell wall permeability and rate of starch digestibility in intact cotyledon cells from four different varieties of pea seeds was studied. Pulsed-field gradient nuclear magnetic resonance (PFG NMR) coupled with light and confocal microscopy were employed to evaluate the cotyledon cells' diffusion coefficients and cell wall permeability. The cotyledon cells' diffusion coefficients and cell wall permeability followed a decreasing trend: White/yellow pea > Marrowfat pea > Maple pea > Blue pea. The varying size of internal cavities in the microstructure in the cotyledon cells, as observed by the light and confocal micrographs, may be responsible for this trend. The extent of starch hydrolysis recorded from the cotyledon cells followed the same trend of the cell wall permeability except for Blue pea cotyledon cells. Thus, indicating that the more permeable the cotyledon cell to the starch-degrading enzymes, the higher the extent of intracellular starch hydrolysis. The microstructure changes in the cotyledon cells during digestion also confirmed this observation.

1. Introduction

Consumption of whole pulse food had been associated with a reduced risk of obesity, type II diabetes, cardiovascular disease and high nutritional value (protein)(Fardet & Boirie, 2014, Marsh et al., 2011 and Wang et al., 2019). This is partly due to its low postprandial glycaemic response. The mechanism of how pulse foods exhibit the low postprandial glycaemic response has been attributed to the ability of the cell structure as well as protein matrix to act as a physical barrier to diffusion of enzymes to the intracellular starch granules in cotyledon cell (Dhital et al., 2016, Bhattarai et al., 2017 Junejo et al., 2021, Do et al., 2019 and Berg et al., 2012). Also, the densely packed crystalline structure retained in the cotyledon cells after cooking limits the swelling and gelatinization of entrapped starch granules (Xiong et al., 2019). The effect of cell wall components and protein matrix on the degree of starch digestibility in pulse cotyledon cells has been studied (Edwards et al., 2021, Huang et al., 2021; Junejo et al., 2021, Li et al., 2019, Rovalino-Córdova et al., 2018; Rovalino-Córdova et al., 2019). It was observed from the various studies that the cotyledon cell wall is the primary barrier that modulate the extent of intracellular starch digestibility in cells by regulating the ingress of water and starch-degrading enzymes. Therefore, an intensive study on the cell wall of the cotyledon cell is imperative to help food processors design functional food ingredients/products from pulses such as low glycaemic index features food (Food that can regulate the release of glucose into the blood stream when ingested).

Cotyledon cell walls mainly consist of cellulose (30 %), xyloglucan (30 %) and pectin (35 %) (Burton et al., 2010 and Voragen et al., 2009). The extent of diffusion of starch degrading enzymes through the cotyledon cell wall is likely to be influenced by numerous factors including cell wall composition and density, cell wall thickness, cellular integrity, the number and size of cell wall pores and processing conditions (Rovalino-Córdova, et al., 2018, Grundy et al., 2016, Junejo et al., 2021 and Pallares Pallares et al., 2019). Rovalino-Córdova, et al. (2018) and Junejo et al. (2021) observed the effect of damaged cellular integrity of cotyledon cell wall on the starch hydrolysis (in vitro) in the pulse cells. They reported that an increase in the damage to the cellular integrity is inversely proportional to the starch hydrolysis in the cell. That is, a reduction in the cellular integrity of the cell will increase the exposure of the intracellular starch to digestive enzymes, thus, increasing starch digestibility. On the other hand, Xiong, et al. (2019) reported that the permeability of pinto bean cotyledon cells was damaged after high-moisture treatment (HMT), thus increasing the extent and rate of intracellular starch digestibility. The porosity /permeability of the cotyledon cell walls has also been studied by other authors by using

* Corresponding author at: School of Food Technology and Natural Sciences, Massey University, Private Bag 11 222, Palmerston North 4442, New Zealand.
E-mail address: J.X.Singh@massey.ac.nz (J. Singh).

https://doi.org/10.1016/j.foostr.2024.100381
Received 12 March 2024; Received in revised form 24 July 2024; Accepted 1 August 2024
Available online 2 August 2024

fluorescein labelled dextran to evaluate the porosity/permeability of cotyledon cell wall when subjected to the different molecular weights of Fluorescein isothiocyanate (FITC)-dextran solutions (Huang et al., 2021, Li et al., 2019 and Li et al., 2019). Fluorescence recovery after photobleaching (FRAP) has also been reported to have been used as verifying microscopy tool with FITC-dextran to observe wall porosity in red kidney cotyledon cells (Li et al., 2019). However, FRAP/FITC-dexran techniques only provide local diffusivity/local fraction data i.e. local diffusion measurement on a micrometres scale on a bleached region of the cotyledon cells (Moud, 2022).

Pulse gradient field -Nuclear magnetic resonance (PFG NMR) has been highlighted as a technique for measuring direct characteristics of transfer in plant systems, such as the coefficients of diffusion, permeability, and water flow rate (Anisimov, 2021 and Watanabe & Fukuoka, 1992). It has been used to provide non-invasive globalized diffusion measurements in soybean seed, carrot and onion tissue and chlorella sp. (Watanabe et al., 1994, Cho et al., 2003, Ando et al., 2009 and Voda et al., 2012).

Compared to FRAP techniques, PFG NMR provides globalised diffusion data over a large domain i.e. macroscopic diffusion data due to the fact that the whole material is subjected PFG NMR measurement, thus resulting often in average diffusion value (Pihl et al., 2018).

Considering this, we hypothesize that the application of PFG NMR to isolated intact cotyledon cells would provide globalized diffusion measurements of its cell wall properties such as diffusion coefficient and cell wall permeability. In our previous study, we investigated the influence of seed microstructure on the hydration kinetics and in-vitro starch digestion of 4 New Zealand pea varieties (Ajala et al., 2022). We reported that pea microstructure parameters such as thickness of the pea seed cell wall and average size of starch granules per cell correlated positively with the hydration kinetics and starch digestion. In order to obtain further insight into the pea microstructure of New Zealand varieties, isolated cotyledon cells were extracted for this study.

Therefore, we evaluated the diffusion coefficient and cell wall permeability of isolated cotyledon cells from the 4 pea seed varieties using PFG NMR and investigated the role of the cell permeability on the intracellular starch granules 'gelatinization and in vitro digestion characteristics.

2. Material and methods

2.1. Material

White/yellow pea (WP), Blue Pea (BP), Maple pea (MP) and Marrowfat pea (MFP) dry pea varieties were used for this study (Cates Grain and Seed Ashburton, New Zealand). Each pea variety was vacuum sealed and stored at 4 ∘C until further studies Amyloglucosidase (3260 U/mL) and alpha-amylase (3000 U/mL) were supplied from Megazyme International Ireland Ltd. (Wicklow, Ireland). invertase (Invertase, grade VII from baker's yeast, 401 U/mg solid), Pepsin (porcine gastric mucosa, 800–2500 U/mg protein) and pancreatin (hog pancreas, 4 × USP) were all from Sigma–Aldrich Ltd. (St Louis, USA). All other chemicals were of analytical grade.

2.2. Isolation of cotyledon cells from the pea seed varieties

Raw pea seed varieties were treated with acid and alkali solutions according to the method described by Kugimiya (1990) and Do et al. (2019) with slight modifications. Briefly, raw pea seeds were soaked in a 0.1 M hydrochloric acid (HCl) solution (pH ~ 1.3) at room temperature for 24 h. The seed coats were removed manually, the resulting cotyledons were rinsed with Reverse Osmosis (RO) water repeatedly to remove the excess acid, then soaked in a 0.06 M sodium hydroxide (NaOH) solution (pH ~ 12.5) in Schott bottles. These bottles were shaken in an orbital shaker at 150 rpm and at room temperature for 24 h. The resulting softened cotyledon was gently minced (set at the min speed) using a fine mincer screen (Kenwood MG700 series). The resulting paste was passed through a stack of 150 and 53 μm sieves under running RO water repeatedly. The cotyledon cells were collected on the 53 μm sieve, freeze-dried and stored at room temperature until further use.

2.3. Morphological properties

2.3.1. Light microscopy

The cotyledon cells of each variety were mounted onto a glass slide, and a drop of water is added and sealed with coverslips. The images were viewed under a Zeiss Axiophot light microscope (LM) with Differential Interference Contrast (DIC) optics and a colour CCD camera (ZEISS microscopy, Germany) using 20x magnification, respectively.

2.3.2. Microstructural characterization

The raw and digested cotyledon cells samples were spread on a scanning electron microscope stub and then gold coated (Baltec SCD 050 sputter coater, New York, USA). The resulting gold-coated stub was viewed using the FEI Quanta 200 Environmental Scanning Electron Microscope (Oregon, USA) at an accelerating voltage of 20 kV.

2.3.3. Particle size distribution

Cotyledon cells were mixed with water to obtain homogeneous suspensions that were then added into a small volume sample dispersion unit (Hydro 2000S) until an obscuration level of ~15 ± 5 % was obtained. Refractive indices of 1.530 and 1.330 were used for cotyledon/blended flour and water phases respectively. Particle size distribution was measured with a laser diffraction particle size analyzer (Malvern Mastersizer 2000; Malvern Instruments Ltd., UK).

2.3.4. Confocal characterization of the cells

The confocal characterization of the cotyledon cells was carried out according to the method described by Li et al. (2020). Briefly, 5 mg cells were dispersed in 300 μL of Fluorescein isothiocyanate FITC solution (1 mg/mL) in a microcentrifuge tube at 4 °C overnight under the dark condition. The suspension was centrifuged at 2000 g and then rinsed several times with Milli-Q water to remove the excess dye. The FITC-stained cotyledon cells were transferred into the glass slide, and a drop (~2 μL) of calcofluor-white stain solution was added. The glass slide was covered with the coverslip. The fluorescence emitted by the samples was collected at 405 nm excitation wavelength for calcofluor white and 488 nm for FITC respectively. Leica SP5 DM6000B scanning confocal microscope (Leica, Germany) was used to observe the morphological features of cotyledon cells.

2.4. Cell wall permeability experiment

2.4.1. Sample preparation

A representative of the freeze-dried cotyledon cells from Section 2.2 was rehydrated as follows. The cotyledon cells were soaked in RO water for 2 h at room temperature, then centrifuged at 4200 rpm (878 g-forces) (Multifuge 1S-R, Thermofisher Scientific, USA) for 30 min after which the supernatant water is removed. The centrifugation process is repeated for another 30 min. This resulted in a thick paste of soaked cells with negligible free water.

2.4.2. PFG NMR diffusion measurement

The PFG NMR method used for this study was described by Ando et al. (2009) with minor modifications. Each variety of centrifuged cotyledon cells was packed into a 5 mm NMR tube. PFG NMR experiments were made at 298 K using a Bruker Avance 500 MHz spectrometer (Bruker Scientific Instruments, Billerica, Massachusetts USA) with a 5 mm QXI probe equipped with a 50 G cm −1 gradient coil a. The standard Bruker pulse program *stebpgp1s* was used., the gradient strength, g, ranged from 5 to 40 G cm-1 with 16 steps. The little delta was constant at 1.5 ms and the big delta varied between 30 ms and 1250 ms.

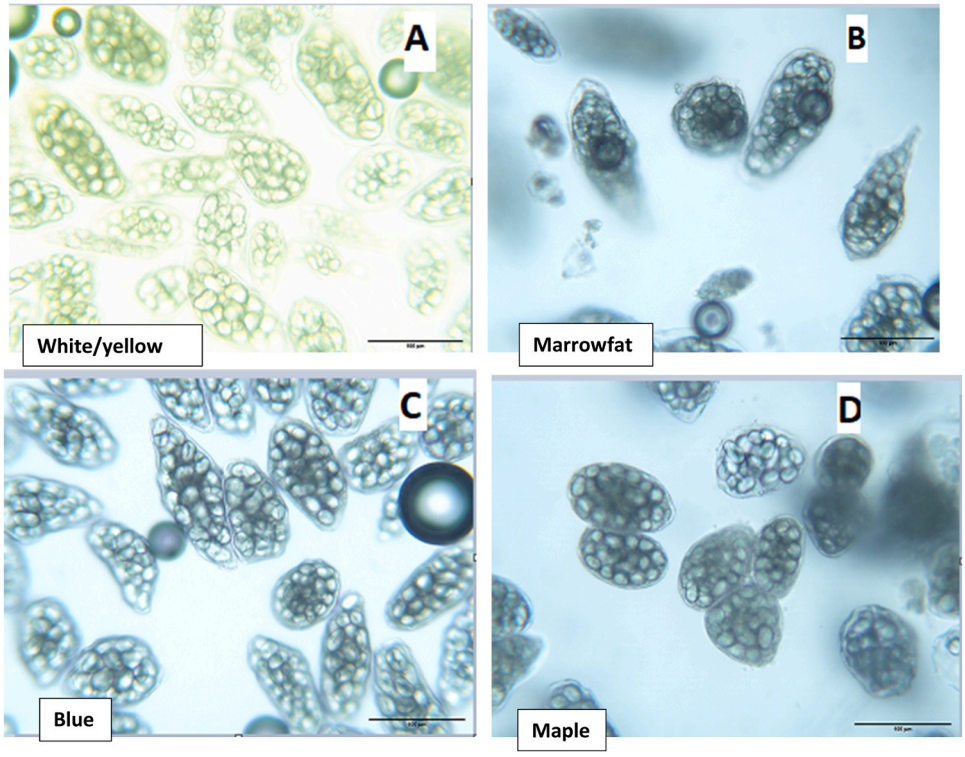

Fig. 1. Light microscopy of pea cotyledon cells Where A, B, C and D are White/yellow, Marrowfat, Blue and Maple cotyledon cells respectively.

Measurements were made over varying diffusion times (30 −1250 ms). Spectra were processed and diffusion constants (D) were extracted by fitting spectra using the Stejskal-Tanner Equation (Stejskal & Tanner, 1965) with Bruker's Topspin 2.1.8 software using standard parameters.

The permeability of the cotyledon cell wall was estimated by the structural model below:

$$1/D_{\infty} = 1/D_0 \quad + 1/(P \times a)$$

Where D_{∞}= Diffusion coefficient at diffusion time 1250 msD_0 = Diffusion coefficient at diffusion time 30 ms$P$ = Permeability of the cell wall$a$ = cotyledon cell size.

2.5. Nutritional composition of the cotyledon cells

The moisture content of the freeze-dried cotyledon cells samples was determined by an air oven drying method at 108 °C (AOAC, 2012). Subsequently, the contents of crude protein and crude fat in pea varieties were analyzed by the Kjeldahl method using a conversion factor of 6.25 from nitrogen to protein and the Mojonnier method respectively (AACC, 2000 and AOAC, 2012). The acid/alkali hot extraction method (AOAC, 2012) was used to quantify the fibre content of cells while the gravimetric method which involved heating the cells sample at 600 °C for 3 hr was used to determine the ash content (AACC, 2000). The carbohydrate contents of the cell samples were estimated via calculation by subtracting the summation of all other components from 100%. All experiments were conducted in triplicate.

The total starch content of the cell samples was analyzed using a total starch assay kit (KTSTA, Megazyme International Ireland Ltd., Ireland) following the manufacturer's instructions. Results were reported on a dry weight basis (%).

2.6. Thermal properties

Thermal properties were evaluated using a Differential Scanning Calorimeter (DSC) (TA Q100, TA Instruments, Newcastle, DE) according to the method described by Edwards et al. (2020) with slight adjustments. Approximately 4 mg of cotyledon cells were weighed into stainless steel pans and water was added at a ratio of water to flours of 3:1. The pans were sealed, and an empty steel pan was used as a reference sample. The samples were heated from 20 °C to 110 °C at 10 °C/min. Onset temperature (T_o), peak temperature (T_p), conclusion temperature (T_c), and enthalpy of gelatinization (ΔH_{gel}) were calculated using Universal Analysis Software (version 4.5 A, TA Instruments).

2.7. X-ray diffraction (crystallinity)

X-ray diffraction analysis was conducted using an X-ray diffractometer (D8 Advance, Bruker, Germany), which was operated at 40 kV and 40 mA with Cu Kα radiation (λ = 0.154 nm). The cotyledon cells were scanned from 4° to 40° (2θ) at a speed of 2°/min and a step size of 0.02°. The relative crystallinity was calculated as the ratio of the crystalline peak area to the total diffraction using EVA 4.2 software (Bruker, Germany).

2.8. In vitro gastro-small intestinal digestion of the cotyledon cells

Cotyledon cells were mixed with water in a ratio of 1:5(w/v) in a Schott bottle to obtain a heterogeneous mixture containing approximately 4% of starch concentration. The resulting mixture was cooked in a hot water bath at 95∘C for 20 min and immediately cooled down in a pre-set water bath at 37 ∘C.

The gastro-small intestinal in vitro digestion model used for this study was described by Dartois et al.(2010). Approximately 170 g of cooked cotyledon cells were introduced into the jacketed glass reactor. The reactor temperature was maintained at 37 ± 1 ∘C by circulating water in the reactor jacket. The reactor contents were mechanically stirred by a magnetic stirrer bar at 300 rpm throughout digestion. The pH was initially adjusted to 2.0 (using 3 M HCl solution), then 25 mL of Simulated Gastric Fluid (SGF) (pepsin: starch ratio of 1.765:100, w/w) was added to start the hydrolysis, and the final pH was adjusted to 1.2 (using 0.5 HCl solution). After 30 min, the pH was adjusted to 6.8 to

Table 1
Particle size analysis of the cotyledon cells.

Cotyledon cells	D (0.1) μm	D (0.5) μm	D (0.9) μm	Mean Diameter (μm)	Specific surface area (m2/g)	Yields (%)
White/yellow	78.91 ± 0.14a	128.8 ± 0.24a	205.0 ± 0.46a	135.3 ± 0.27a	0.06 ± 0.12a	19.8
Marrowfat	79.14 ± 1.85a	145.5 ± 0.44c	264.3 ± 1.32c	146.1 ± 2.41b	0.06 ± 0.01a	12.7
Blue	91.61 ± 1.69b	140.8 ± 0.41b	217.0 ± 3.89a	146.7 ± 0.27b	0.05 ± 0.03b	16.8
Maple	90.34 ± 0.11b	148.6 ± 0.10d	245.6 ± 0.37b	146.5 ± 0.13b	0.04 ± 0.02c	18.2

[a, b, c] Values in each column with the same superscript letters are not significantly different ($p > 0.05$).

inactivate the pepsin enzyme. Subsequently, 22 mL of Simulated Intestinal Fluid (SIF) (pancreatin/starch ratio, 1.3:100, w/w, amyloglucosidase/starch ratio, 0.26:1, v/w, and invertase/starch ratio, 1:1000, w/w) was added to start the small intestinal digestion, and pH was maintained at 6.8 using 0.5 and 3 M NaOH solution. The total time to complete the gastric and small-intestinal digestion was 30 and 120 min, respectively.

A 0.5 mL of aliquot was withdrawn from the reactor after 0, 15, and 30 min of gastric digestion (G0, G15, and G30), and 0, 5, 10, 15, 30, 60,90, and 120 min of the small intestinal digestion (I0, I5, I10, I15, I30, I60, I90, and I120). The glucose concentration of the incubated mixture was measured using the D-glucose assay kit (GOPOD Format K-GLUK 07/ 11, Megazyme International Ireland Ltd, Ireland).

Starch hydrolysis was expressed in percentage as described by Dartois et al. (2010).

$$\%SH = 0.9 \quad x \quad \frac{Gp}{Si}$$

Where %SH is the percentage of starch hydrolysis, Gp is the glucose produced, and Si is the initial amount of starch. Starch hydrolysis on the isolated cotyledon cell was conducted in triplicates.

2.9. Statistical analysis

The mean and standard deviation were evaluated for all reported values except those stated otherwise. All values were subjected to statistical analysis (One-way ANOVA) using Minitab 19.1.1.0 statistical software (Minitab LLC, Chicago, USA) at $p \leq 0.05$.

3. Results and discussion

3.1. Microstructural characterization of isolated intact cotyledon cells from pea varieties

The cotyledon cells isolated for this study showed high cellular integrity and minimal starch gelatinization as shown in Fig. 1. This result agrees with the other authors that the acid/alkali pre-treatment method for isolating cotyledon cells produces intact cells with negligible free starch granules or broken cell walls (Dhital et al., 2016 ; Kim & Kim, 2015). During successive acid-alkali solution treatment isolation methods, the polyvalent metal ions connecting the cells are separated by the acid, while the solubilization of pectin with β-elimination reaction is promoted by the alkali (Aguilera et al., 2001; Kugimiya, 1990). The total yield (Table 1) of the isolated cotyledon cells for this study is less than 20% (dry matter) which is within the range reported in the literature (Bhattarai et al., 2017 and Pälchen et al., 2021, Pälchen et al. 2021). The low yield of isolated cotyledon cells from different isolation methods available in literature established the fact that detailed insight into the relationship between isolation techniques and the total yield of cotyledon cells is urgently needed (Ajala et al., 2023). It was observed that the large amount of residue generated during the sieving procedure contain large clusters of cotyledon cells as shown in Fig. 8.

In general, all cotyledon cell samples (Fig. 1) appear to be elongated, ellipsoidal, or spherical with sizes ranging from 130 to 150 μm (Table 1). The particle size of the cotyledon cells from white/yellow pea varieties was a significant difference ($P < 0.05$) from the other varieties and it

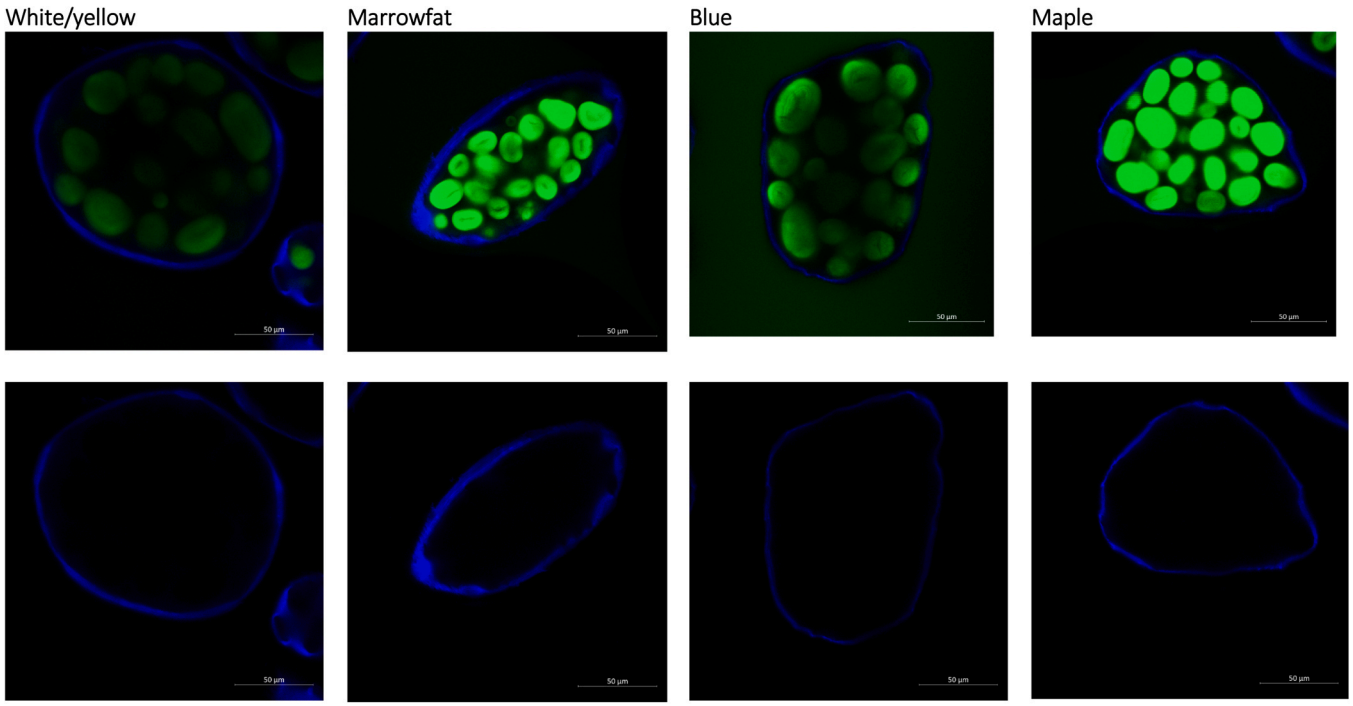

Fig. 2. Confocal characterization of pea cotyledon cells(top row) and highlighted cell walls(bottom row). Where, WP, MFP, BP and MP cotyledon cells are White/yellow, Marrowfat, Blue and Maple cotyledon cells respectively.

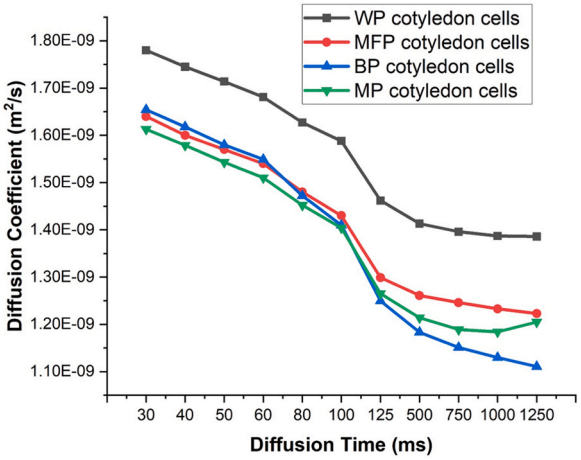

Fig. 3. The measured diffusion coefficient of water in intact cotyledon cells as a function of diffusion time. Where, WP, MFP, BP and MP cotyledon cells are White/yellow, Marrowfat, Blue and Maple cotyledon cells respectively.

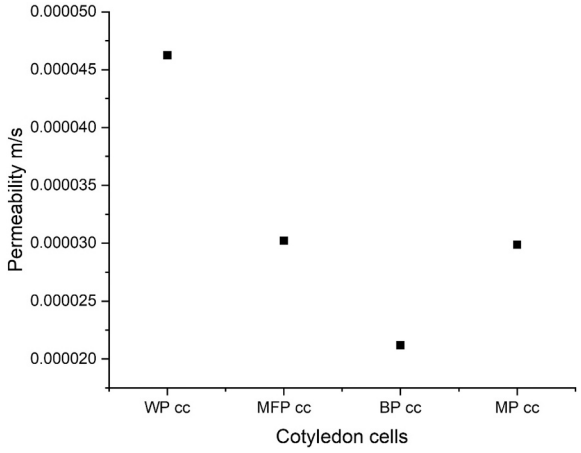

Fig. 4. Permeability of the intact cotyledon cells. Where, WP, MFP, BP and MP cotyledon cells are White/yellow, Marrowfat, Blue and Maple cotyledon cells respectively.

seems the specific surface area decreases with an increased mean diameter (Table 1). The starch granules for all the isolated cotyledon cells are shown to be densely packed within the boundaries of the cell walls (Fig. 1 & **2**). There are distinct internal cavities that are obvious with the starch granules as shown in Fig. 2. Such cavities have been reported by other authors (Li et al., 2019; Li et al., 2018). These distinct cavities indicate the negligible effect of the acid/alkali pre-treatment isolation techniques on the intracellular starch granules (limited starch gelatinization) due to the high level of cellular integrity as exhibited by the intact cell wall (Fig. 2).

3.2. Diffusion experiment of the cotyledon cells using PFG NMR

The diffusion coefficient of water in all the cotyledon cells decreased with increased diffusion time (Fig. 3**)**. At the beginning of the diffusion experiment, WP cotyledon cells exhibited a higher diffusion coefficient than cells from the other varieties. Similarly, when the diffusion time is in the 80 ms, the diffusion coefficient shown by WP cotyledon cells was twice as much as that of the other cotyledon cells. At the end of the diffusion experiment (diffusion time = 1250 ms), the diffusion coefficient of all the cotyledon cells followed a trend; WP > MFP>MP>BP. Overall, between the diffusion time of 30 to 1250 ms, BP cotyledon cells exhibited the highest decrease in diffusion coefficient compared to other cotyledon cells. The trend of the diffusion coefficient decreasing with increased diffusion time for this study is consistent with the other authors (Cho et al., 2003 and Ando et al., 2009). The diffusion coefficient of water in a cell is a quantitative measure of the molecular movement of water in and out of the cell (Kitamura & Kinjo, 2018). There are three main mechanisms for water transportation in plants system: namely (a). Intracellular water self-diffusion in a cell; (b) molecular diffusion of water between adjacent cells and groups of cells; and (c) long-distance transport associated with the mass flow of water between the organs of the plant (Anisimov, 2021). For this study, the diffusion of water into the cotyledon cells can be ascribed to the first mechanism. The light and confocal micrographs (Fig. 1 &**2**) showed the cotyledon cells are largely separated with negligible aggregates of cells, thus reducing the effect of the second mechanism described above. The diffusion behavior for this study exhibited restricted diffusion, that is, water molecules cannot freely move in the cotyledon cells due to a barrier such as a cell wall or cell membrane (Ando et al., 2009). Therefore, BP-isolated cotyledon cells exhibited more restricted diffusion compared to the other cells.

The water permeability of the intercellular barrier (cotyledon cell wall) as estimated by Eqt 1, showed that the isolated cotyledon cells followed a decreasing trend; WP > MFP >MP > BP (Fig. 4). That is, the water permeability tends to be highest and lowest in WP and BP cotyledon cells respectively. It is assumed that the cell wall in BP cotyledon cells is less porous than in WP cotyledon cells. The permeability reported for this study is larger than fresh onion tissue but consistent with freeze-thawed onion tissue reported by other authors (Ando et al., 2009). The larger permeability exhibited by the cotyledon cells for this study can be attributed to the irreversible distorted functionality of the native microstructure of the cell wall caused during the freeze-drying process (Voda et al., 2012). The ice crystals are formed from the intracellular water in the cell during the rapid freeze stage and they sublime via the pores of the cell wall, thus leaving behind a more porous cell. Even after rehydration of the cells in water as described in this study, the native functionality of the cell wall cannot be recovered (Aravindakshan et al., 2021 and Voda et al., 2012). The freeze-drying of the cotyledon cells sample was mandatory for this study because it's an efficient drying method (more than 95% of water is removed and the cells were microbiologically stable) which is an important pre-requisite for the diffusion experiment for this study. To limit the effects of freeze-drying on the microstructure integrity of the cotyledon cells, other drying methods such fluid-bed drying could be explored in further studies.

Furthermore, pulse seed cell walls are made up of type I primary cell walls that are rich in xyloglucans and pectic polysaccharides. The interactions between these polymers form an assembly of complex

Table 2
Nutritional composition of the cotyledon cells in dry weight basis.

Cotyledon cells	Moisture (%)	Protein (%)	Fat (%)	Fibre (%)	Ash (%)	Carbohydrate (%)	Total starch (%)
White/Yellow	10.03 ± 0.12^{b}	14.61 ± 0.37^{a}	0.53 ± 0.16^{a}	2.65 ± 0.12^{a}	0.49 ± 0.13^{a}	71.69 ± 0.66^{c}	55.23 ± 0.58^{b}
Marrowfat	9.27 ± 0.31^{a}	21.93 ± 0.14^{d}	0.56 ± 0.19^{a}	3.61 ± 0.33^{d}	0.85 ± 0.06^{c}	63.78 ± 0.38^{a}	51.63 ± 1.34^{a}
Blue	9.63 ± 0.29^{ab}	16.46 ± 0.24^{b}	0.48 ± 0.21^{a}	2.94 ± 0.19^{b}	0.73 ± 0.02^{b}	69.75 ± 0.59^{b}	63.44 ± 0.59^{c}
Maple	11.23 ± 0.06^{c}	20.25 ± 0.05^{c}	0.25 ± 0.13^{b}	3.37 ± 0.47^{c}	0.82 ± 0.09^{c}	64.08 ± 0.49^{a}	54.67 ± 0.38^{b}

[a, b, c] Values in each column with the same superscript letters are not significantly different ($p > 0.05$).

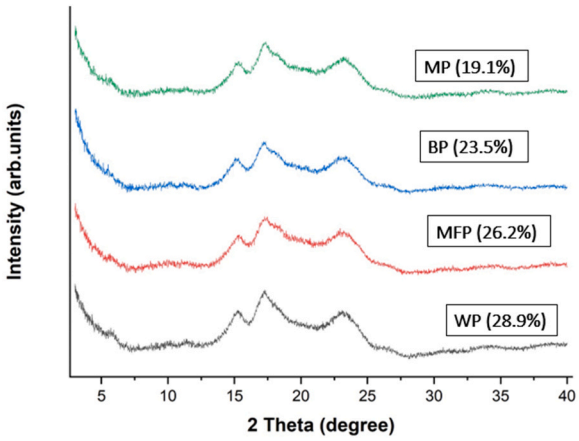

Fig. 5. Relative crystallinity of cotyledon cells. Where, WP, MFP, BP and MP cotyledon cells are White/yellow, Marrowfat, Blue and Maple cotyledon cells respectively.

macromolecular structures that regulate the apoplastic cellular exchange of macromolecules such as enzymes, protein water and gas (Rondeau-Mouro et al., 2008 and Edwards et al., 2021). The acid/alkali extraction condition used for isolating the cotyledon cells for this study may limit intracellular starch granules gelatinization in the cell, the cell wall architecture had been reported to be modified via swelling, breakage of hydrogen bonds and drastic chemical structure modification (Rondeau-Mouro et al.,2008). This could also be responsible for the large water permeability results reported for the study.

Now, a direct comparison of the diffusion data obtained via PFG NMR for isolated cotyledon cells for this study with FRAP/FITC techniques used on cotyledon cells by other authors (Huang et al., 2021, Li et al., 2019a and Li et al., 2019b) would be difficult because of the different probes used by both techniques (Pihl et al., 2018). Water as used in this study or pegylated molecules are used as probe for PFG NMR techniques while FITC-dextran of different molecular weights are used as probe for FRAP methods.

3.3. Nutritional composition of the cotyledon cells

The proximate composition of the cotyledon cells for this study tends to be significantly different among the pea varieties ($p < 0.05$) (Table 2**).** The protein content of the cotyledon cells tends to increase from WP <BP<MP<MFP. The fat content on the other hand among the cotyledon cells from the pea varieties was less than 1%. This low-fat content from the cotyledon cells is expected and consistent with other reports (Bhattarai et al., 2017). The fibre content of the cells differs significantly among the pea varieties ($p < 0.05$) and followed the same trend with the protein content. The total starch value available in cells (Table 2) seems to be the most abundant component (total starch content for all cells > 50%). The cotyledon cells from blue pea varieties showed a starch content 10% more than the cells from the other varieties. This total starch content agrees with the other authors (Pälchen et al., 2021). The nutritional composition of the cotyledon cells for this study identified the significant presence of starch, protein, and fibre components. These components are validated with the distinct starch granules, protein bodies and cellular materials (cell wall) as observed from the light microscope (Fig. 1), Confocal image (Fig. 2) and SEM micrograph (Fig. 7), thus indicating functionality of the cell such as cell wall porosity, starch gelatinization and digestibility would depend on these components.

3.4. Crystallinity and thermal properties

The x-ray diffraction results and total relative crystallinity for the intracellular starch granules in the cotyledon cells from different pea varieties were illustrated in Fig. 5**.** The XRD pattern of the intracellular starch granules in the cotyledon cell samples presented characteristics of a C-type polymorphic pattern (mixture of A- and B type of X-ray pattern) with major peaks at 5.6°, 11.5°, 15.4°, 17.6°, and 23.6° 2theta. The X-ray diffractograms for this study are consistent with the report by other authors (Junejo et al., 2021). The total relative crystallinity of the entrapped starch granules of the cotyledon cells samples was less than 30% and increase from MP<BP<MFP< WP. These results fall within the range reported by other researchers (Junejo et al., 2021 ; Li et al., 2020). The disruption of the crystalline structure of starch granules in the cotyledon cells and the permeability of the cotyledon cell wall tend to follow a similar trend (Li et al., 2023).

Table 3
Thermal properties of the cotyledon cells.

Cotyledon cells	T_o (°C)	T_p (°C)	T_c (°C)	ΔH_{gel} (J.g-1)
White/yellow	56.45 ± 1.05[b]	63.64 ± 2.09[b]	97.26 ± 1.78[b]	8.83 ± 1.58[a]
Marrowfat	54.17 ± 0.89[a]	64.71 ± 1.41[a]	95.70 ± 3.96[c]	18.13 ± 3.46[c]
Blue	58.52 ± 0.10[c]	64.65 ± 0.69[a]	95.46 ± 2.99[c]	8.06 ± 1.51[a]
Maple	55.96 ± 0.58[ab]	62.80 ± 0.02[c]	98.84 ± 0.76[a]	10.64 ± 0.70[b]

[a, b, c] Values in each column with the same superscript letters are not significantly different ($p > 0.05$) where.
Onset temperature (T_o), peak temperature (T_p), conclusion temperature (T_c), and enthalpy of gelatinization (ΔH_{gel}) respectively.

The thermal properties of the cotyledon cells reported for this study (Table 3) showed that all cotyledon cells exhibited a single endothermic transition with broad peaks from 54 to 98 ∘C, which reflected delayed gelatinization. The onset temperature (T_o), peak temperature (T_p), conclusion temperature (T_c), and enthalpy of gelatinization (ΔH_{gel}) for this study were consistent with those reported in the literature (Li et al., 2019, Do et al., 2019 and Li et al., 2023). The onset temperature (T_o) of the starch granules in the cotyledon cells for the study differ significantly among the varieties ($p < 0.05$). The onset temperature (T_o) of the entrapped starch granules in the cells increases in the following trend: MPF<MP<WP<BP. The peak temperature (T_p) and conclusion temperature (T_c) values of the intracellular starch granules in MFP and BP cotyledon cells do not differ significantly. The delayed entrapped starch

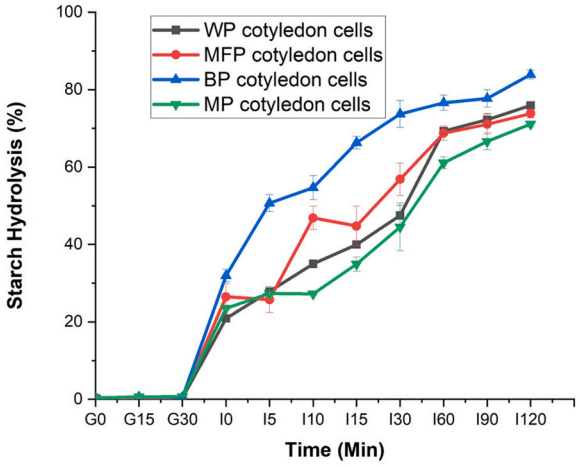

Fig. 6. Starch hydrolysis of the cotyledon cells during in vitro gastro-small intestinal digestion. Where, WP, MFP, BP and MP cotyledon cells are White/yellow, Marrowfat, Blue and Maple cotyledon cells respectively. G0, G15, and G30 (0, 15, and 30 min of gastric digestion), and I0, I5, I10, I15, I30, I60, I90, and I120 (0, 5, 10, 15, 30, 60,90, and 120 min of the small intestinal digestion).

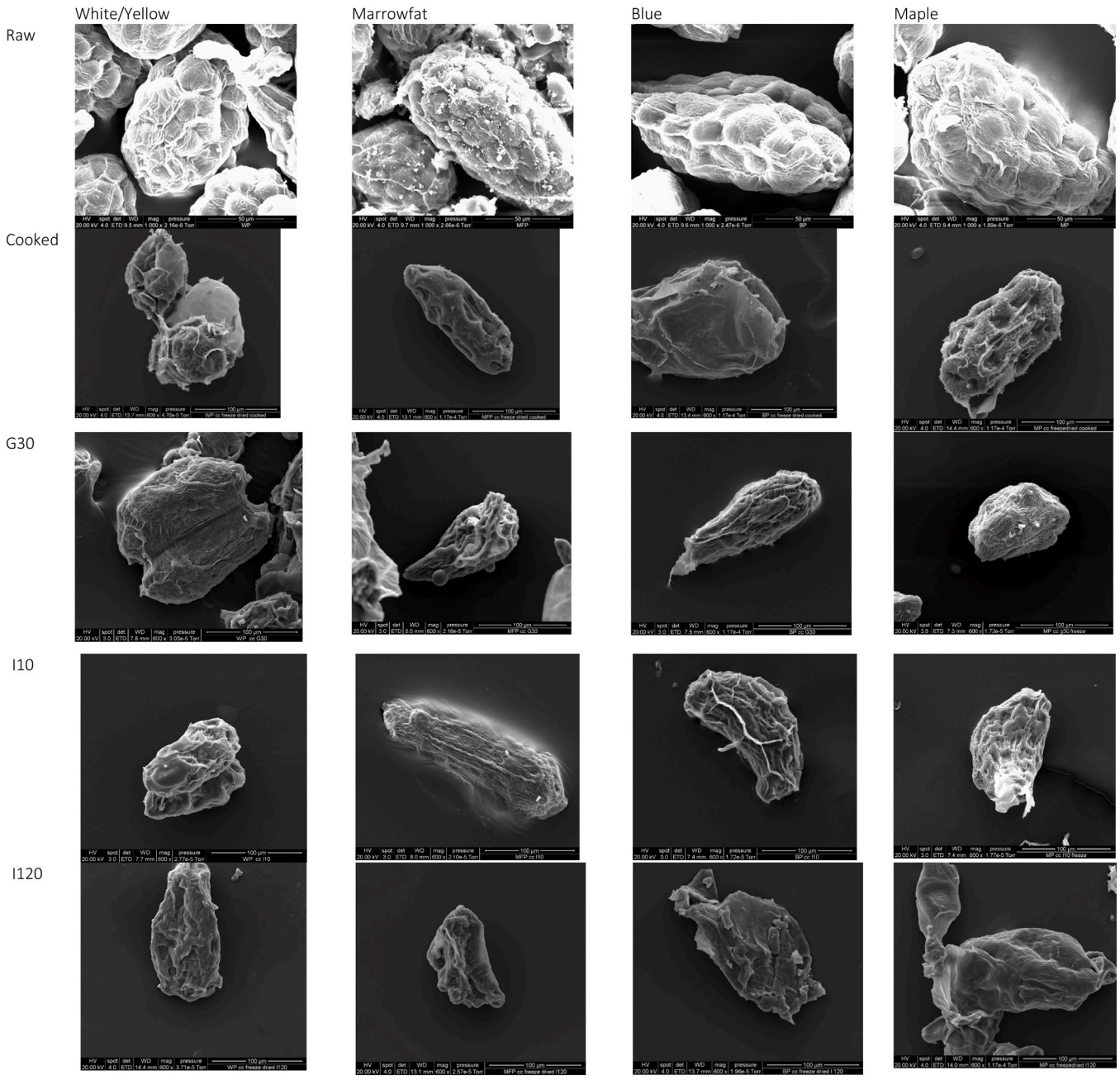

Fig. 7. Scanning electron micrographs of cotyledon cells samples isolated from four pea varieties (White/yellow pea, Marrowfat pea, Blue pea and Maple pea) during in vitro gastro and small intestinal digestion. Where G30 is gastric digestion at 30 min while I10 and 1120 are small intestinal digestion at 10 and 120 min respectively.

gelatinization in the cells reported for the reflected the degree of permeability of the cell wall earlier reported in this study do regulate the inflow of water into the cell, thereby limiting the degree of starch gelatinization.

The enthalpy of gelatinization (ΔH_{gel}) for this study (Table 3) showed a significant difference in value between the MFP and MP cotyledon cells while the starch granules in WP and BP cells do not differ significantly in their enthalpy of gelatinization value. ΔH_{gel} can predict the energy required to break down the intermolecular hydrogen bonds of the amylopectin crystallites in legumes starch granules (Hoover et al., 2010 and Ahmed et al., 2021). This implies that the energy required to provide the order-disorder transition of starch granules in both WP and BP cotyledon cells respectively is similar. On the other hand, the starch granules in MFP required more energy than MP.

3.5. *In vitro gastro-intestinal starch digestion of cotyledon cells*

In vitro gastro-small, intestinal digestion of the cooked cotyledon cells is illustrated in Fig. 6. As expected, no starch hydrolysis occurred at the gastric stage because of the absence of starch-degrading enzymes (α-amylase) in the simulated gastric fluid (SGF). For the small intestinal digestion, after 10 min, the starch hydrolysis of all the cotyledon cells was between the range of 27.25–54.46%. The starch hydrolysis of the cooked cotyledon cells then moved sharply to the range of 44.52–73.71% after 30 min. After 90 mins, the starch hydrolysis in MP cotyledon cells was 10 times less than the other cotyledon varieties. The starch hydrolysis then rose steadily until the end of 120 min of the small intestinal starch digestion. Overall, the final starch hydrolysis of the cooked cotyledon cells ranges between 71.1–83.8%. The MP and BP

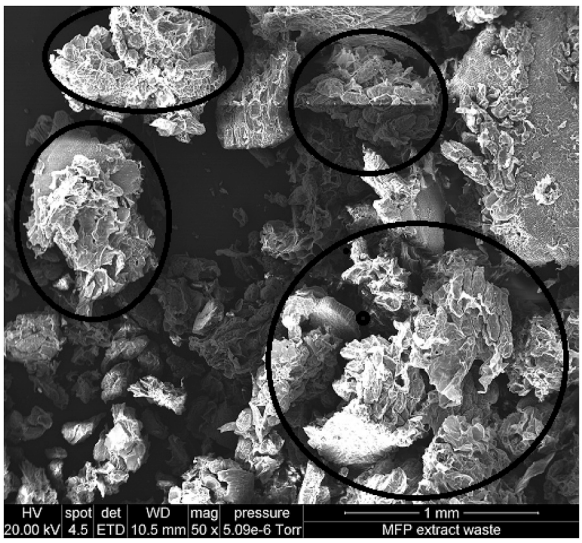

Fig. 8. Scanning electron micrograph of the waste generated during cotyledon cell isolation. Note. The circle indicated large clusters of cotyledon cells.

cotyledon cells recorded the lowest and highest starch hydrolysis, respectively (Fig. 6).

The starch hydrolysis of the cotyledon cells for this study was lower than the reported value from other authors (Junejo et al., 2021, Li et al., 2020) but was consistent with some other researchers (Do et al., 2019 and Rovalino-Córdova et al., 2019). The discrepancy between the starch digestibility in the cotyledon cells for this study and other authors could be attributed to the effect of processing treatment on the structural modification in the cotyledon cell wall (Rondeau-Mouro et al.,2008). It is imperative to note that, the cotyledon cells that tend to show lower starch digestibility from other reports were subjected to more heating (cooking) at the isolation stage and before the starch digestion procedure than the cotyledon cells for this study. This is important because literature has reported that the structure type I primary cell wall (Xyloglucan and pectic polysaccharides) of pulse cotyledon cells exhibit high cellular integrity after cooking (Berg et al., 2012, and Edwards et al., 2021). Thus, hypothesizing that the reinforcement of pectin-rich polysaccharide polymers in the cell wall from several heating procedures would limit the ingress of starch degrading enzymes in the cell far better.

Nonetheless, the moderately low starch hydrolysis reported amongst the cotyledon cells for this study corroborates the permeability study conducted on the cells. WPF and MFP cotyledon cells that showed large permeability to water (Fig. 4) tend to show high starch hydrolysis (Fig. 6). This implies that, though the molecular weight of water used for the permeability experiment is lower than the digestive enzymes, the porosity of WPF and MFP cotyledon cell walls allowed more ingress of the starch degrading enzymes than MP cotyledon cell during digestion. The BP cotyledon cells, on the other hand, exhibited the highest starch hydrolysis despite having shown to have a cell wall that is less permeable to water (Fig. 4). One of the probable reasons for this could be attributed to the distinct internal cavities observed in the confocal images of the cells (Fig. 2). The internal cavities in the BP cotyledon cells seem to be largely due to the less densely packed starch granules in the cells compared to other cells. What this means is that complete gelatinization (complete swelling and disruption of the crystalline starch granules) of some of the starch granules is possible compared to cotyledon cells.

The overview of the microstructure of the cotyledon cells in their raw state, after cooking, at the end of the gastric phase (G30) and in the small-intestinal digestion stage (I10 & I120) are summarised in Fig. 7. The SEM micrograph of the raw cotyledon cells varied in different shapes and sizes with distinct identifiable densely packed starch granules encapsulated by a cell wall. At the cooking stage, major structural changes such as indentations and wrinkles were observed on the surface of largely intact cotyledon cells. The internal components (intracellular starch and protein bodies) of the cell undergo physicochemical changes (partially gelatinized starch, leached amylose and denatured protein in the presence of heat and water introduced during cooking. At this point, it is important to assume that a drastic structural change had happened to the cotyledon cell wall. A similar observation had been reported by other authors (Do et al., 2019 and Berg et al., 2012). At the end of the gastric stage, there were no distinct changes observed in the cotyledon cell. As the digestion proceed in the small intestine from I10 to I120, numerous indentations and pits were observed on the surface of the cotyledon cells. This could have resulted from the leaching of some digested intracellular molecules during the digestion process. Overall, the cell walls of the cotyledon cells at the end of the digestion process are larger and intact (Fig. 7) with some cotyledon cells exhibiting more collapse structure (multiple layers of folding and shrinking) than others. The degree of drastic microstructural changes that occur in the cotyledon cells from raw to cooked (introduction of water and heat), gastric and small intestinal stages (introduction of starch degrading enzymes) depend on the extent of porosity or permeability of the cell wall Fig. 8.

4. Conclusions

The role of cell wall permeability in the microstructure and the extent of in vitro starch hydrolysis of intracellular starch in cotyledon cells were investigated for this study. The light and confocal micrographs observed a high level of cellular integrity of the cotyledon cells before diffusion experiments. The PFG NMR provided a globalized measurement of the diffusion coefficients of the cell and how its cell wall is permeable to water during the diffusion experiment. The light and confocal micrograph confirmed the trend observed in the cell permeability behavior of the cotyledon cells. The degree of starch hydrolysis buttressed the cell wall permeability trend observed by the PFG NMR. The study provided a fundamental measurement in understanding the role of cell wall permeability in cotyledon cells, however, for a holistic investigation on the cell wall of pulse cotyledon cells, other specific characteristics such as the number and size of cell wall pores should be investigated.

CRediT authorship contribution statement

Jaspreet Singh: Supervision. **Patrick J.B. Edwards:** Methodology. **Abayomi Ajala:** Writing – original draft. **Sung Je Lee:** Supervision. **Lovedeep Kaur:** Supervision.

Declaration of Competing Interest

Authors declare no conflict of interest.

References

AACC. (2000). Approved methods of the American Association of Cereal Chemists. St. Paul, Minn.: American Assoc. of Cereal Chemists,10.01, 30–10, 08–01.01, 51–61 & 76–21.

Aguilera, J. M., Cadoche, L., López, C., & Gutierrez, G. (2001). Microstructural changes of potato cells and starch granules heated in oil. *Food Research International, 34*(10), 939–947. https://doi.org/10.1016/s0963-9969(01)00118-1

Ahmed, J., Mulla, M. Z., Siddiq, M., & Dolan, K. D. (2021). Micromeritic, thermal, dielectric, and microstructural properties of legume ingredients: A review. *Legume Science, 4*(1). https://doi.org/10.1002/leg3.123

Ajala, A., Kaur, L., Lee, S. J., & Singh, J. (2023). Native and processed legume seed microstructure and its influence on starch digestion and glycaemic features: A review. *Trends in Food Science & Technology*. https://doi.org/10.1016/j.tifs.2023.01.011

Ajala, A., Kaur, L., Lee, S. J., & Singh, J. (2022). Influence of seed microstructure on the hydration kinetics and oral-gastro-small intestinal starch digestion in vitro of New Zealand pea varieties. *Food Hydrocolloids, 129*, Article 107631. https://doi.org/10.1016/j.foodhyd.2022.107631

Ando, H., Fukuoka, M., Miyawaki, O., Watanabe, M., & Suzuki, T. (2009). PFG NMR study for evaluating freezing damage to onion tissue. *Bioscience, Biotechnology, and Biochemistry, 73*(6), 1257–1261. https://doi.org/10.1271/bbb.80681

Anisimov, A. (2021). Gradient NMR method for studies of water translational diffusion in plants. *Membranes, 11*(7), 487. https://doi.org/10.3390/membranes11070487

AOAC. (2012). Official Methods. Official methods of analysis of AOAC international (19th ed., Vol. 925). Gaithersburg, Md, USA: AOAC International, 10 & 962.09/978.10.

Aravindakshan, S., Nguyen, T. H., Kyomugasho, C., Buvé, C., Dewettinck, K., Van Loey, A., & Hendrickx, M. E. (2021). The impact of drying and rehydration on the structural properties and quality attributes of pre-cooked dried beans. *Foods, 10*(7), 1665. https://doi.org/10.3390/foods10071665

Berg, T., Singh, J., Hardacre, A., & Boland, M. J. (2012). The role of Cotyledon cell structure during in vitro digestion of starch in navy beans. *Carbohydrate Polymers, 87*(2), 1678–1688. https://doi.org/10.1016/j.carbpol.2011.09.075

Bhattarai, R. R., Dhital, S., Wu, P., Chen, X. D., & Gidley, M. J. (2017). Digestion of isolated legume cells in a stomach-duodenum model: Three mechanisms limit starch and protein hydrolysis. *Food & Function, 8*(7), 2573–2582. https://doi.org/10.1039/c7fo00086c

Burton, R. A., Gidley, M. J., & Fincher, G. B. (2010). Heterogeneity in the chemistry, structure and function of Plant Cell Walls. *Nature Chemical Biology, 6*(10), 724–732. https://doi.org/10.1038/nchembio.439

Cho, C., Hong, Y., Kang, K., Volkov, V. I., Skirda, V., Lee, C. J., & Lee, C. (2003). Water self-diffusion in chlorella sp. studied by pulse field gradient NMR. *Magnetic Resonance Imaging, 21*(9), 1009–1017. https://doi.org/10.1016/s0730-725x(03)00206-6

Dartois, A., Singh, J., Kaur, L., & Singh, H. (2010). Influence of guar gum on the in vitro starch digestibility—Rheological and microstructural characteristics. *Food Biophysics, 5*(3), 149–160. https://doi.org/10.1007/s11483-010-9155-2

Dhital, S., Bhattarai, R. R., Gorham, J., & Gidley, M. J. (2016). Intactness of cell wall structure controls the in vitro digestion of starch in legumes. *Food & Function, 7*(3), 1367–1379. https://doi.org/10.1039/c5fo01104c

Do, D. T., Singh, J., Oey, I., & Singh, H. (2019). Modulating effect of Cotyledon cell microstructure on in vitro digestion of starch in legumes. *Food Hydrocolloids, 96*, 112–122. https://doi.org/10.1016/j.foodhyd.2019.04.063

Edwards, C. H., Ryden, P., Mandalari, G., Butterworth, P. J., & Ellis, P. R. (2021). Structure–function studies of Chickpea and durum wheat uncover mechanisms by which cell wall properties influence starch bioaccessibility. *Nature Food, 2*(2), 118–126. https://doi.org/10.1038/s43016-021-00230-y

Edwards, C., Ryden, P., Pinto, A., Van der Schoot, A., Stocchi, C., Perez-Moral, N., & Ellis, P. (2020). Chemical, physical and glycaemic characterisation of PulseON®: A novel legume cell-powder ingredient for use in the design of functional foods. *Journal of Functional Foods, 68*, Article 103918. https://doi.org/10.1016/j.jff.2020.103918

Fardet, A., & Boirie, Y. (2014). Associations between food and beverage groups and major diet-related chronic diseases: An exhaustive review of pooled/meta-analyses and systematic reviews. *Nutrition Reviews, 72*(12), 741–762. https://doi.org/10.1111/nure.12153

Grundy, M. M., Edwards, C. H., Mackie, A. R., Gidley, M. J., Butterworth, P. J., & Ellis, P. R. (2016). Re-evaluation of the mechanisms of dietary fibre and implications for macronutrient bioaccessibility, digestion and postprandial metabolism. *British Journal of Nutrition, 116*(5), 816–833. https://doi.org/10.1017/s0007114516002610

Hoover, R., Hughes, T., Chung, H., & Liu, Q. (2010). Composition, molecular structure, properties, and modification of pulse starches: A review. *Food Research International, 43*(2), 399–413. https://doi.org/10.1016/j.foodres.2009.09.001

Huang, Y., Dhital, S., Liu, F., Fu, X., Huang, Q., & Zhang, B. (2021). Cell wall permeability of Pinto Bean Cotyledon cells regulate in vitro fecal fermentation and gut microbiota. *Food & Function, 12*(13), 6070–6082. https://doi.org/10.1039/d1fo00488c

Junejo, S. A., Ding, L., Fu, X., Xiong, W., Zhang, B., & Huang, Q. (2021). Pea cell wall integrity controls the starch and protein digestion properties in the INFOGEST in vitro simulation. *International Journal of Biological Macromolecules, 182*, 1200–1207. https://doi.org/10.1016/j.ijbiomac.2021.05.014

Kim, E., & Kim, H. (2015). Physicochemical properties of dehydrated potato parenchyma cells with ungelatinized and gelatinized starches. *Carbohydrate Polymers, 117*, 845–852. https://doi.org/10.1016/j.carbpol.2014.10.038

Kitamura, A., & Kinjo, M. (2018). Determination of diffusion coefficients in live cells using fluorescence recovery after photobleaching with wide-field fluorescence microscopy. *Biophysics and Physicobiology, 15*(0), 1–7. https://doi.org/10.2142/biophysico.15.0_1

Kugimiya, M. (1990). Separation of cotyledon cells of legumes by successive treatments with acid and alkali. *Nippon Shokuhin Kogyo Gakkaishi, 37*(11), 867–871. https://doi.org/10.3136/nskkk1962.37.11_867

Li, H., Gidley, M. J., & Dhital, S. (2019). Wall porosity in isolated cells from food plants: Implications for nutritional functionality. *Food Chemistry, 279*, 416–425. https://doi.org/10.1016/j.foodchem.2018.12.024

Li, P., Dhital, S., Fu, X., Huang, Q., Liu, R., Zhang, B., & He, X. (2020). Starch digestion in intact pulse cotyledon cells depends on the extent of thermal treatment. *Food Chemistry, 315*, Article 126268. https://doi.org/10.1016/j.foodchem.2020.126268

Li, P., Dhital, S., Zhang, B., He, X., Fu, X., & Huang, Q. (2018). Surface structural features control in vitro digestion kinetics of bean starches. *Food Hydrocolloids, 85*, 343–351. https://doi.org/10.1016/j.foodhyd.2018.07.007

Li, P., Zhang, B., & Dhital, S. (2019). Starch digestion in intact pulse cells depends on the processing induced permeability of cell walls. *Carbohydrate Polymers, 225*, Article 115204. https://doi.org/10.1016/j.carbpol.2019.115204

Li, P., Zhang, B., Liu, R., Ding, L., Fu, X., Li, H., & He, X. (2023). Insights into the relations between cell wall integrity and in vitro digestion properties of granular starches in pulse cotyledon cells after dry heat treatment. *Food Science and Human Wellness, 12*(2), 528–535. https://doi.org/10.1016/j.fshw.2022.07.055

Marsh, K., Barclay, A., Colagiuri, S., & Brand-Miller, J. (2011). Glycemic index and glycemic load of carbohydrates in the diabetes diet. *Current Diabetes Reports, 11*(2), 120–127. https://doi.org/10.1007/s11892-010-0173-8

Moud, A. A. (2022). Fluorescence recovery after photobleaching in colloidal science: Introduction and application. *ACS Biomaterials Science & Engineering, 8*(3), 1028–1048. https://doi.org/10.1021/acsbiomaterials.1c01422

Pallares Pallares, A., Loosveldt, B., Karimi, S. N., Hendrickx, M., & Grauwet, T. (2019). Effect of process-induced common bean hardness on structural properties of in vivo generated boluses and consequences for in vitro starch digestion kinetics. *British Journal of Nutrition, 122*(04), 388–399. https://doi.org/10.1017/s0007114519001624

Pälchen, K., Michels, D., Duijsens, D., Gwala, S., Pallares Pallares, A., Hendrickx, M., & Grauwet, T. (2021). *In vitro* protein and starch digestion kinetics of individual chickpea cells: From static to more complex in vitro digestion approaches. *Food & Function, 12*(17), 7787–7804. https://doi.org/10.1039/d1fo01123e

Pälchen, K., Michels, D., Duijsens, D., Gwala, S., Pallares Pallares, A., Hendrickx, M., & Grauwet, T. (2021). *In vitro* protein and starch digestion kinetics of individual chickpea cells: From static to more complex in vitro digestion approaches. *Food & Function, 12*(17), 7787–7804. https://doi.org/10.1039/d1fo01123e

Pihl, M., Kolman, K., Lotsari, Antiope, Ivarsson, M., Schüster, E., Lorén, Niklas, & Bordes, R. (2018). Silica-based diffusion probes for use in FRAP and NMR-diffusometry. *Journal of Dispersion Science and Technology, 40*(4), 555–562. https://doi.org/10.1080/01932691.2018.1472015

Rondeau-Mouro, C., Defer, D., Leboeuf, E., & Lahaye, M. (2008). Assessment of cell wall porosity in Arabidopsis thaliana by NMR spectroscopy. *International Journal of Biological Macromolecules, 42*(2), 83–92. https://doi.org/10.1016/j.ijbiomac.2007.09.020

Rovalino-Córdova, A. M., Fogliano, V., & Capuano, E. (2018). A closer look to cell structural barriers affecting starch digestibility in beans. *Carbohydrate Polymers, 181*, 994–1002. https://doi.org/10.1016/j.carbpol.2017.11.050

Rovalino-Córdova, A. M., Fogliano, V., & Capuano, E. (2019). The effect of cell wall encapsulation on macronutrients digestion: A case study in kidney beans. *Food Chemistry, 286*, 557–566. https://doi.org/10.1016/j.foodchem.2019.02.057

Stejskal, E. O., & Tanner, J. E. (1965). Spin diffusion measurements: Spin echoes in the presence of a time-dependent field gradient. *The Journal of Chemical Physics, 42*(1), 288–292. https://doi.org/10.1063/1.1695690

Voda, A., Homan, N., Witek, M., Duijster, A., Van Dalen, G., Van der Sman, R., & Van Duynhoven, J. (2012). The impact of freeze-drying on microstructure and rehydration properties of carrot. *Food Research International, 49*(2), 687–693. https://doi.org/10.1016/j.foodres.2012.08.019

Voragen, A. G., Coenen, G., Verhoef, R. P., & Schols, H. A. (2009). Pectin, a versatile polysaccharide present in plant cell walls. *Structural Chemistry, 20*(2), 263–275. https://doi.org/10.1007/s11224-009-9442-z

Wang, M., Wichienchot, S., He, X., Fu, X., Huang, Q., & Zhang, B. (2019). In vitro colonic fermentation of dietary fibers: Fermentation rate, short-chain fatty acid production and changes in microbiota. *Trends in Food Science & Technology, 88*, 1–9. https://doi.org/10.1016/j.tifs.2019.03.005

Watanabe, H., & Fukuoka, M. (1992). Measurement of moisture diffusion in foods using pulsed field gradient NMR. *Trends in Food Science & Technology, 3*, 211–215. https://doi.org/10.1016/0924-2244(92)90193-z

Watanabe, H., Fukuoka, M., & Shimada, S. (1994). Measurement of moisture diffusion in a soybean seed by pulsed-field-gradient NMR method. *Developments in Food Engineering*, 236–238. https://doi.org/10.1007/978-1-4615-2674-2_71

Xiong, W., Zhang, B., Dhital, S., Huang, Q., & Fu, X. (2019). Structural features and starch digestion properties of intact pulse cotyledon cells modified by heat-moisture treatment. *Journal of Functional Foods, 61*, Article 103500. https://doi.org/10.1016/j.jff.2019.103500